

## Microstructural Study of Strong Vortex Pinning in a Coated Conductor for Use in Specific Fields and Temperatures

Fumitake Kametani, Zhijun Chen, Alex Gurevich and David Larbalestier  
Applied Superconductivity Center, National High Magnetic Field Laboratory, Florida State University, Tallahassee, FL32301

Yimin Chen, Yi-Yuan Xie and Venkat Selvamanickam  
SuperPower Inc. Schenectady, NY 12304

**Abstract**— It is still unclear what type, size, shape and distribution of defects and nano particles in a coated conductor are optimum for specific temperatures and fields. Cross-sectional transmission electron microscope has been performed to study the microstructure of the YBCO films and coated conductors (CCs) with defects and nano particles and its correlation of vortex pinning at various temperature and fields. The MOCVD CC we examined contains dense ab-plane stacking faults and three-dimensional  $Y_2O_3$  nanoprecipitates. We also made PLD YBCO films containing  $Y_2O_3$  nanoprecipitates of smaller size and spacing. Although the volume fraction of  $Y_2O_3$  is comparable (~12-15%), the MOCVD CC shows higher  $H_{irr}$  at 77 K, indicating stronger resistance to thermal fluctuations at high fields. However, deconvolution of the strong and weak pinning components of the pinning indicates a crossover at lower temperatures where the PLD film with smaller nanoprecipitates shows stronger pinning. We are attempting to incorporate thermal fluctuation effects into our description of the optimum pinning nanostructures.

### I. INTRODUCTION

Since YBCO films were aimed for practical application in the form of coated conductor, various effective pinning structures – especially addition of nano particles – have been proposed [1-3]. However it is still unclear what type, size, shape and distribution of defects and nano particles in a coated conductor are optimum for specific temperatures and fields. Cross-sectional transmission electron microscope (TEM) has been performed to study the microstructure of YBCO films and coated conductors (CCs) with defects and nano particles of different size, shape and distribution so as to make correlation to vortex pinning at various temperature and fields. Here we compare a home-grown multi-layer PLD sample with a commercial MOCVD CC, both of which contain dense ab-plane stacking faults and three-dimensional  $Y_2O_3$  or (Y, Sm) $_2O_3$  nanoprecipitates. The PLD YBCO film contains  $Y_2O_3$  nanoprecipitates of smaller size and spacing than those in the MOCVD CC. Although the volume fraction of  $Y_2O_3$  is comparable (~12-15%), the MOCVD CC shows higher  $H_{irr}$  at 77 K, indicating stronger resistance to thermal fluctuations at high fields. However, deconvolution of the strong and weak pinning components of the pinning derived from analysis of the Jc-T curves over a wide range of H and T using the Barcelona group approach [1] indicates a crossover at lower temperatures where the PLD film with smaller nanoprecipitates shows stronger pinning. This crossover indicates that thermal fluctuation effects should be taken into

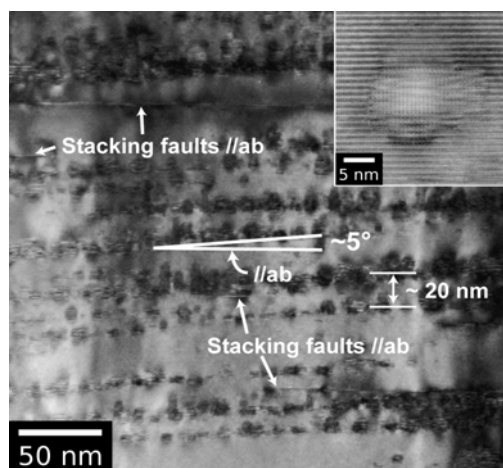


Figure 1 Cross-sectional TEM image of the MOCVD CC showing the  $Y_2O_3$  nano precipitate arrays and stacking faults. The typical HREM of precipitate is shown in the inset.

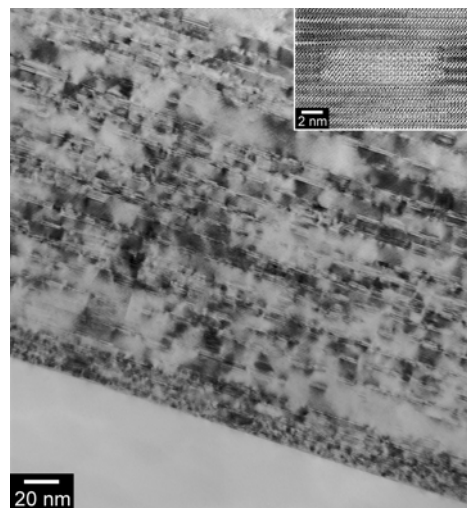


Figure 2 Cross-sectional TEM image of the PLD YBCO film showing  $Y_2O_3$  precipitates of smaller size and spacing. The inset HREM shows the typical shape of the precipitate.

account for description of the optimum pinning nanostructures.

Sample	T <sub>c</sub> (K)	J <sub>c</sub> (77K, sf)	J <sub>c</sub> (10K, sf)	H <sub>irr</sub> (77K)	ppt thick-ness (nm)	ppt spacing along ab-plane (nm)	ppt spacing along c-axis (nm)	Vol%
MOCVD 2μm thick CC	90.8	3.82	38.4	8.8T	~8nm	~10-20	non-uniform ~20-50	13%
PLD 0.6μm thick	90.1	4.21	48	6.8T	~3nm	~20	~10	15%

Table 1

II. RESULTS AND DISCUSSION

A cross-sectional TEM image of the MOCVD CC is shown in Fig.1. The black dot contrasts represent the (Y, Sm)<sub>2</sub>O<sub>3</sub> nano precipitates of ~8x15 nm in size as shown in the inset HREM image. The strain field contrast can be seen on the top and bottom of the precipitates. It may extend the effective size of the pinning center. Y<sub>2</sub>O<sub>3</sub> preferentially aligns in 10~20 nm spacing along the horizontal direction at a 5° tilt away from the ab-plane, forming precipitate arrays, whose spacing of ~20-50 nm along the c-axis is not uniform. The image also shows ab-plane stacking faults, another major pinning defect. The volume fraction of Y<sub>2</sub>O<sub>3</sub> measured with ImageJ software is ~13 %.

Fig.2 shows a cross-sectional TEM image of the PLD YBCO film. Y<sub>2</sub>O<sub>3</sub> nano precipitates were found as well as the MOCVD CC. Y<sub>2</sub>O<sub>3</sub> in this film also preferentially aligns along ab-plane in ~20 nm spacing. The inset HREM shows that the typical size of Y<sub>2</sub>O<sub>3</sub> is ~3x10 nm, smaller than that in the MOCVD CC. The volume fraction of Y<sub>2</sub>O<sub>3</sub> is ~15 % resulting in smaller spacing of ~10 nm along c-axis and higher density compared to the MOCVD CC. The inset HREM also indicates that, despite the semi-coherency of Y<sub>2</sub>O<sub>3</sub> and YBCO, less strain field is visible around precipitates because of its smaller size.

Table 1 briefly summarizes the basic properties and microstructure of those two samples. Although T<sub>c</sub> and the volume fraction of precipitates are comparable, H<sub>irr</sub>(77K) of MOCVD CC is more enhanced than that of the PLD YBCO, while self-field J<sub>c</sub> of the PLD YBCO is higher at both 77K and 10K, beyond explanation by 0.7K T<sub>c</sub> difference.

To investigate more details of the pinning, deconvolution of the strong and weak pinning components was derived from analysis of the J<sub>c</sub>-T curves over a wide range of H and T using the Barcelona group approach [1], partly shown in Fig.3. Striking is that a crossover of the strong pinning component occurs around 40K at 8T indicating greater pinning enhancement in the PLD YBCO at low temperature and high field, although H<sub>irr</sub>(77K) of the MOCVD CC is more enhanced as shown in the inset. According to the model of Gurevich et al [4], thermal fluctuation of vortices becomes greater especially near H<sub>irr</sub> as temperature increases. Comparing the size and distribution of precipitates in Table 1 indicates that, when thermal fluctuations diminish at low temperatures, the pin density becomes dominant rather than the pin size. However we need the strong separated pins – precipitates in bigger size and spacing in this case – to chop vortices into short segment at 77K near H<sub>irr</sub>, indicating that

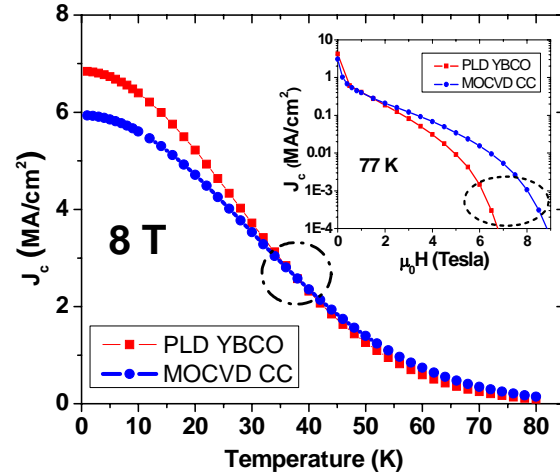


Figure 3 The strong pinning component of the pinning at 8 T, while the inset shows J<sub>c</sub> vs H at 77 K. A crossover occurs around 40K at 8T.

we need to optimize the pinning nanostructure taking thermal fluctuation into account at each T and H.

III. CONCLUSION

We compared the nanostructure of pins in the MOCVD CC and PLD YBCO film both of which have the Y<sub>2</sub>O<sub>3</sub> nano precipitates of the similar volume fraction but in a different size and distribution. Deconvolution of the strong and weak pinning components of the pinning from analysis of the J<sub>c</sub>-T curves over a wide range of H and T showed a crossover of the strong pinning component at high T and H where we need the precipitates in bigger size and larger spacing at 77K near H<sub>irr</sub>. Our results suggest that we must take the thermal fluctuation effect into account to optimize the pinning nanostructure at each T and H.

ACKNOWLEDGMENT

This work was supported by SuperPower Inc., by the Air Force Office of Scientific Research, and by the US Department of Energy.

REFERENCES

[1] J. Gutierrez et al. *Nature Mat.*, **6**, 367-373, 2007  
 [2] T. Haugan et al. *Nature* **430**, 867-870, 2004  
 [3] J. L. Macmanus-Driscoll et al. *Nature Mat.* **3**, 439-443, 2004  
 [4] A. Gurevich et al., *Supercond. Sci. Technol.* **20**, S128, 2007